Superchron cycles driven by variable core heat flow

P. Driscoll[1,2] and P. Olson[1]

Received 17 January 2011; revised 21 March 2011; accepted 30 March 2011; published 4 May 2011.

[1] A numerical dynamo with time variable core heat flow and inner core growth rate links the thermal state of the Earth's core to the long term trends in the Geomagnetic Polarity Time Scale (GPTS). Increasing core heat flow over 100 Myr drives the numerical dynamo from a superchron state to reversing behavior, whereas a similar decrease in core heat flow produces a decrease in reversal frequency, driving the dynamo back into a superchron. The polarity sequence, including more than 400 reversals and two superchrons, compares favorably with the GPTS, as does the dynamo frequency spectrum. We find that core heat flow is positively correlated with polarity reversal frequency, dipole variability, and the relative strength of the non-dipole field. Our results imply that changes in geomagnetic reversal frequency can be attributed to long period fluctuations in core heat flow, and suggest heat flow minima during superchrons and a maximum near the present-day. **Citation:** Driscoll, P., and P. Olson (2011), Superchron cycles driven by variable core heat flow, *Geophys. Res. Lett.*, *38*, L09304, doi:10.1029/2011GL046808.

1. Introduction

[2] The Geomagnetic Polarity Time Scale shows a progressive increase in the average frequency of magnetic polarity reversals since the end of the most recent superchron in the late Cretaceous [*Cande and Kent*, 1995; *Gallet and Courtillot*, 1995; *Constable*, 2000], when no polarity reversal occurred over a period of ~40 Myr. Other long term modulations in reversal frequency, including one or possibly two earlier superchrons, have been identified at approximately 200 Myr intervals [*Gallet et al.*, 1992; *Pavlov and Gallet*, 2005]. Numerical dynamo models have successfully reproduced many features of geomagnetic polarity reversals, including the irregular timing of individual polarity events and the collapse of the dipole component of the field [*Amit et al.*, 2010]. However, these models have yet to address the main secular trend of the GPTS: a decrease in reversal frequency going back to the end of the Cretaceous Normal Superchron (CNS) 83 Ma, no reversals during the CNS 83–120 Ma, and increasing reversal frequency prior to 120 Ma. Statistical models [*Ryan and Sarson*, 2007] explain variations in reversal frequency including superchrons in terms of log-normal or other asymmetric probability distributions arising from a stationary process. However, statistical models do not account for the observed trends in reversal frequency between superchrons, and their main assumption of a stationary geodynamo is questionable in light of the fact that mantle structure evolves significantly over a superchron cycle.

[3] The observed cycling of paleomagnetic polarity reversal frequency from superchron to reversing state with a time scale of approximately 200 Myr [*Pavlov and Gallet*, 2005] is comparable to the time scale of convective turnover in the mantle $t_{conv} = \pi D/U \approx 200$ Myr, where D is the mantle thickness and the mean sea floor spreading rate $U =$ 45 mm yr^{-1} represents the convective mantle velocity. This suggests that these two processes may be coupled, which is consistent with numerical models of mantle convection that predict core heat flow variations on similar time scales [*Nakagawa and Tackley*, 2005; *Zhong et al.*, 2007]. Here we demonstrate using a numerical geodynamo model how modest temporal variations in total core heat loss of about 25% can drive the geodynamo into and out of superchrons, accounting for the long term trends in the GPTS reversal frequency.

2. Methods

[4] We model dynamo action in a rotating, convecting, electrically conducting fluid shell with the present-day geometry of Earth's core using the numerical dynamo code MAGIC (developed by J. Wicht). To control the convective forcing, we use the co-density formulation for temperature and composition [*Aubert et al.*, 2009] and specify the strengths of buoyancy production in the fluid and the buoyancy flux on the outer boundary. A time-dependent, spatially uniform heat flux relative to the heat conducted down the core adiabat is specified on the outer boundary, whereas the inner boundary has fixed co-density. Although it has been found that the CMB heat flow pattern can influence magnetic field morphology, numerical dynamos show that polarity reversal rates are more sensitive to changes in the mean CMB heat flow than changes in its planform [*Olson et al.*, 2010]. In the fluid, buoyancy production is represented by a uniform volumetric sink term that represents the combined effects of light element enrichment of the outer core due to solidification of the inner core, curvature of the adiabat, radioactive heating, and secular cooling of the outer core [*Driscoll and Olson*, 2009a].

[5] Two superchron regimes occupy the first and last 20 Myr of the simulation when the core heat flux is adiabatic and convection is driven solely by compositional buoyancy released at the inner core boundary (ICB). The superchrons are separated by a 20–100 Myr phase with a steady increase in superadiabatic core heat flux and polarity reversal frequency, and a 100–180 Myr phase with a steady decrease in superadiabatic core heat flux and polarity reversal frequency (Figure 1c). The first 100 Myr represents the evolution of the geodynamo from the middle of the Cretaceous Normal Superchron (CNS) to its present-day state; the second 100 Myr reverses the trend, similar to the paleomagnetic record between 200 and 100 Ma. The choice of adiabatic

[1]Earth and Planetary Science, Johns Hopkins University, Baltimore, Maryland, USA.
[2]Now at Geology and Geophysics, Yale University, New Haven, Connecticut, USA.

0094-8276/11/2011GL046808

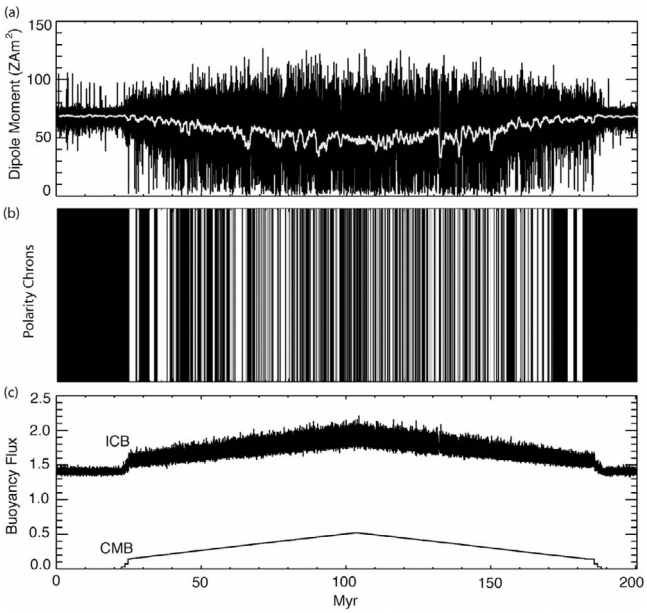

Figure 1. Reversing numerical dynamo over 200 Myr. (a) Variations of dipole moment (black) and with 1 Myr smoothing (white) scaled to the Earth ($Z \equiv 10^{21}$). (b) Polarity chrons; normal (black) and reversed (white). (c) Variations of dimensionless buoyancy flux F at the ICB (top) and CMB (bottom).

heat flow during superchrons is not unique because the parameters are far from realistic and there are a large number of dimensionless parameters that influence dynamo behavior, but the net increase in buoyancy flux (~25%) is necessary to evolve the dynamo from superchron to frequently reversing behavior.

[6] Computational requirements of the 3D numerical dynamo dictate low resolution (l, m = 42 harmonics) and large Ekman number to simulate 200 Myr of continuous core evolution. Dimensionless control parameters include the Ekman number $E = \nu/\Omega D^2 = 5.5 \times 10^{-3}$, Prandtl number $Pr = \nu/\kappa = 1$, magnetic Prandtl number $Pm = \nu/\lambda = 20$, and Rayleigh number $Ra = g\Delta C D^3/\kappa\nu = 2.5 \times 10^4$, where ν, κ, and λ are the viscous, thermochemical, and magnetic diffusivities, Ω is rotation rate, D is shell thickness, and g is gravity. The co-density $C = \alpha T + \beta\chi$ is the fractional change in density associated with perturbations in temperature T and light element concentration χ, where α and β are the thermal and compositional expansivities. Mechanical boundary conditions are no slip at both boundaries, and the inner core has the same electrical conductivity as the outer core, while the mantle is insulating. Time in these calculations is calibrated in units of the magnetic dipole free decay time, which is approximately 20 kyr for a core conductivity of 5×10^5 S m^{-1} (see auxiliary material).[1]

3. Results

[7] The 200 Myr dynamo time series (Figure 1) includes variations of the dipole moment (Figure 1a) and the stable polarity chron stripes (Figure 1b) associated with 421 model polarity reversals. To compare the dynamo to the geomagnetic field we use a scaling law [*Christensen and Aubert*, 2006] to convert the model dipole moment to physical units [*Driscoll and Olson*, 2009a], yielding a time average and standard deviation of the dipole moment of 60 ± 19 ZAm^2 ($Z \equiv 10^{21}$), slightly less than the inferred Virtual Axial Dipole Moment (VADM) paleointensity of 67 ± 34 ZAm^2 for the last 160 Ma [*Tauxe and Yamazaki*, 2007]. The smoothed dipole moment (white, Figure 1a) has a minimum of ~50 ZAm^2 when the core heat flux is largest at 100 Myr, only 17% below its long term average, whereas the total magnetic field intensity at the CMB (not shown) displays an even smaller trend over time. This is consistent with some paleomagnetic measurements which indicate little trend in paleointensity over the last 160 Myr [*Tarduno et al.*, 2001; *Tauxe and Yamazaki*, 2007]. Interestingly, our model predicts increased variability and non-dipole field intensity during periods of frequent reversals (see below), adding to the difficulty of extracting small dipole moment trends from paleointensity measurements.

[8] The superadiabatic thermo-chemical buoyancy flux (Figure 1c) is prescribed at the CMB (F_{CMB}) as a heat flux condition, whereas F_{ICB} is a combination of thermal and chemical buoyancy and fluctuates dynamically. Note that large amplitude steps in F_{CMB} are used for the transition from the adiabatic state to the super-adiabatic state, which dictates that the superchrons are 40 Myr in total length. *Hulot and Gallet* [2003] have proposed that the onset of a superchron occurs suddenly, possibly driven by rapid changes in the CMB heat flow due to small scale convection in D″ [*Olson et al.*, 1987], but previous calculations indicate it is possible to evolve from a superchron to reversing state with a smoothly varying buoyancy flux [*Driscoll and Olson*, 2009a]. We note that the accelerated rate of core evolution used in previous models to explore the dependence of reversal frequency on buoyancy flux [*Driscoll and Olson*, 2009a] is not employed here. In the model, dynamo evolution crosses the regime boundary separating dipolar reversing and non-reversing dynamos, but because the model is not in the same region of parameter space as Earth's core we assume that a similar boundary also exists in the Earth-like region of parameter space.

[9] The polarity reversals in Figure 1 occur when the dipole field collapses and the dipolarity (relative strength of the dipole to total field intensity) is anomalously low; a robust feature of reversing numerical dynamos [*Amit et al.*, 2010]. Physically, increased buoyancy flux invigorates convection in the outer core, causing distortion of the large scale magnetic field. This additional distortion results in weakening of the dipole field and a proliferation of regions that have reversed magnetic flux, precipitating more frequent polarity reversals.

[10] The expanded segment of the dynamo record between 95 and 100 Myr (Figure 2) contains 23 polarity reversals (~4.5 Myr^{-1}) corresponding to the 0–5 Ma reversal rate in the GPTS. The segment also contains 25 excursions (when the dipole axis crosses the equator briefly before returning to the old polarity) often occurring near polarity chron boundaries, but several isolated events can be seen around 99 Myr. Similar to paleointensity records of the last 5 Myr [*Valet et al.*, 2005], each polarity reversal and excursion event is associated with a local minimum in dipole moment of ~10 ZAm^2. This segment also contains two longer chrons, one with reverse polarity from 96.7 to 97.7 Myr, another with normal

[1] Auxiliary materials are available in the HTML. doi:10.1029/2011GL046808.

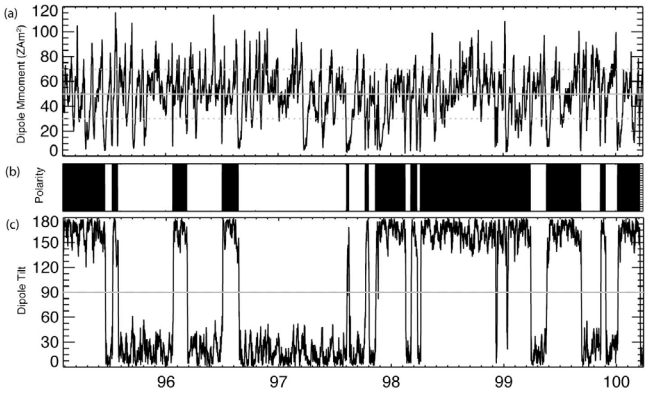

Figure 2. Reversing portion of the dynamo model from 95–100 Myr. (a) Dipole moment (black), with mean (grey) and standard deviation about the mean (grey dashed). (b) Polarity chrons; normal (black) and reversed (white). (c) Dipole tilt colatitude.

polarity from 98.3 to 99.2 Myr, analogous to the present-day Brunhes chron, which is three times longer than the average chron length over the last 5 Myr. The presence of chrons 2–3 times longer than average chron length indicate that quiet periods like the Bruhnes chron may not be so anomalous.

[11] The entire polarity chron record from the dynamo model (cut and shifted to align the superchrons with the CNS) displays randomness in the timing of individual reversals, as well as overall shortening of chron length away from the superchron, similar to the GPTS (Figure 3). In addition, the average polarity reversal rate of the dynamo smoothed with Gaussian kernels [*Constable*, 2000] compares well with the paleomagnetic average (Figure 4a). *McFadden and Merrill* [1997] suggest that there may be an asymmetry in the reversal rate before and after the CNS, which is pronounced in Figure 4a after the superchron where the paleomagnetic reversal rate is lower than the model. However, the model reversal rate is symmetric around the superchron, indicating that an asymmetric reversal rate is likely attributable to differences in core heat flux before and after the CNS.

[12] In general, long chrons have large mean dipole intensity and low variability, indicating they are relatively stable to dipole collapses, while shorter chrons have weak mean dipole intensity and large variability, indicative of their relative instability (Figure 4b), but this trend is scattered for short chrons. The positive correlation between paleomagnetic dipole variability and intensity in the Oligocene, spanning chron lengths of 0.05–2 Myr [*Constable et al.*, 1998], appear similar to the scattered short chron behavior of the model where a positive correlation may be drawn (see auxiliary material). At longer chrons the model seems to have the opposite trend of the paleomagnetic data, although a comparison is difficult here because there are only two paleomagnetic data points with dipole intensities >25 μT. On the contrary, paleomagnetic segments from 49.5–46.5 Ma and 325–310 Ma are examples of periods when reversals were infrequent, dipole intensity was high, and variability was low [*Biggin and Thomas*, 2003]. A larger compilation of paleomagnetic data of various chron lengths could resolve the trend in Figure 4b, and provide an additional means of comparing the model with the geodynamo. Significantly, both the dynamo model and paleomagnetic data contain no chrons with low variability (~5 μT) and moderate dipole intensity (~25 μT).

[13] Observations of paleosecular variation from the Jurassic and Cretaceous indicate increased dispersion of the geomagnetic pole during times of frequent polarity reversals [*Biggin et al.*, 2008]. If increased dipole dispersion is indicative of a broader instability in the dipole field then these observations may be attributed to an increase in the variability of the dipole accompanying frequent reversals, as demonstrated here.

[14] The dispersion of chron length versus chron number (Figure 4c) reflects the fact that reversal frequency is anti-correlated with chron length, and that the range of chron lengths (excluding the superchrons) span at least an order of magnitude from ~20 kyr to ~1 Myr. The two superchron states appear as outliers; some statistical models also infer the CNS to be an outlier [*Hulot and Gallet*, 2003; *Ryan and Sarson*, 2007; *Jonkers*, 2007], but these models do not account for systematic trends in reversal frequency between superchrons. The dipole component of the magnetic field is highly variable and weak during short polarity chrons (~0.03 Myr), contributing less than 40% of the total field, whereas during longer chrons (~1 Myr) the dipole and non-dipole field components are roughly equal (Figure 4d). This suggests that geomagnetic dipole moment (GDM) determinations from periods with frequent reversals are more likely to be contaminated by non-dipole field components, whereas GDM measurements during the CNS may be less affected. Correcting the GDM record with an estimate of the amount of non-dipole contamination as a function of chron length may alter the standard interpretation [*Tauxe and Yamazaki*, 2007] that there is little trend over the last ~160 Myr.

[15] The dipole moment frequency spectrum from the dynamo is compared with various geomagnetic spectrum estimates [*Constable and Johnson*, 2005; *Valet et al.*, 2005; *Courtillot and Le Mouel*, 1988] in Figure 5. The spectra have similar shape with a large slope at high frequencies, a plateau at moderate frequencies associated with polarity reversal fluctuations, and largest power at low frequencies. The decrease in power at high frequency is associated with secular variation and is not well resolved in the dynamo for $f \geq 100$ Myr^{-1}, but the slope is broadly consistent with f^{-2}. The jump in dynamo spectral power near $f = 0.05$ Myr^{-1} is associated with the two superchrons, and the peak power at 100 Myr corresponds to the periodicity of the CMB heat flux forcing. We note that using advective time scaling

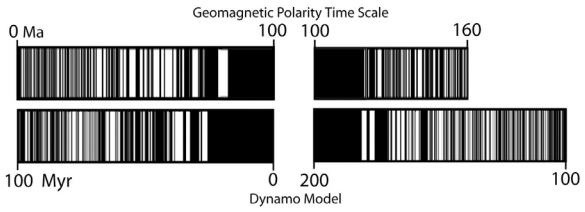

Figure 3. (top) Geomagnetic Polarity Time Scale sea floor record 0–160 Ma [*Lowrie and Kent*, 2004] (bottom) compared to dynamo polarity record 0–200 Myr. Black (white) is normal (reverse) polarity. For comparison purposes the dynamo record has been cut and shifted so that its superchrons align with the CNS.

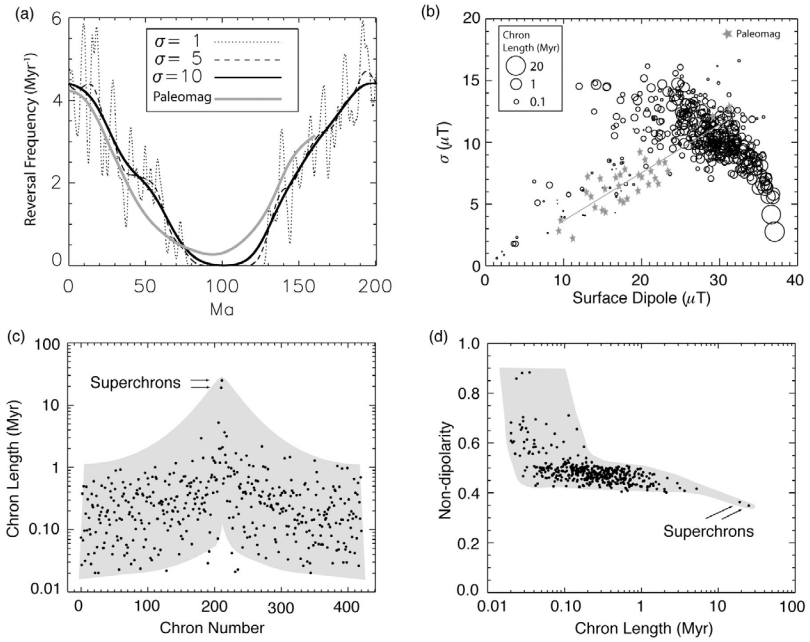

Figure 4. Comparison of paleomagnetic and numerical dynamo reversal properties. (a) Average polarity reversal frequency $R(\mathrm{Myr}^{-1})$ with Gaussian smoothing (standard deviations σ = 1, 5, and 10 Myr). Over-plotted is the smoothed geomagnetic polarity reversal rate for 0–160 Ma [*Constable*, 2000]. For comparison purposes the dynamo model has been shifted the same as in Figure 3. (b) Scaled mean surface dipole intensity versus its standard deviation σ for each stable polarity chron, with symbol sized by chron length, compared to paleomagnetic data [*Constable et al.*, 1998] (stars). (c) Dispersion of polarity chron length versus chron number. (d) Correlation between mean CMB non-dipolarity within chrons and chron length. Non-dipolarity $n = (B - B_d)/B$ measures the normalized contribution of all non-dipole field components, where B and B_d are the total and dipole field rms magnetic field at the CMB, respectively.

(instead of dipole decay time) to generate the dynamo frequency spectra will shift the spectra to higher frequency, and would necessitate an even longer simulation to model the lowest frequencies.

4. Conclusions

[16] Our results support earlier suggestions that paleomagnetic reversal frequency variations may correlate with long-term fluctuations in heat loss from the core [*Courtillot and Le Mouel*, 1988]. Our dynamo model demonstrates that increased heat loss energizes convection in the outer core, destabilizing the axial dipole field by increasing its variability, leading to more frequent polarity excursions and reversals. Previous studies [*Roberts and Glatzmaier*, 2001; *Driscoll and Olson*, 2009a, 2009b; *Aubert et al.*, 2009] estimate that the slowing of Earth's rotation rate due to tidal friction tends to compensate for the decrease in buoyancy production associated with the secular cooling of the core, producing little change in long-term magnetic field strength or average reversal rate. However, our results suggest that geodynamo evolution into and out of superchrons is indicative of dynamical fluctuations in core heat flow, as predicted by whole mantle convection models [e.g., *Nakagawa and Tackley*, 2005; *Zhong et al.*, 2007]. In the future, progresses in modeling the long-term reversal behavior of the geodynamo in combination with more detailed paleomagnetic reversal records prior to 160 Ma may allow for the energetic state of the geodynamo to be used as an additional constraint on the history of the deep Earth.

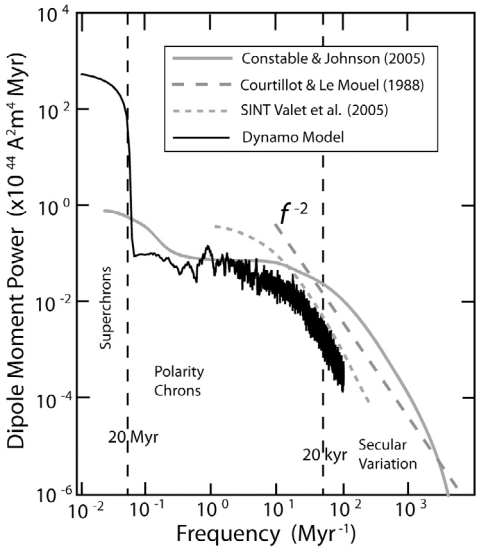

Figure 5. Comparison of dipole moment frequency spectrum from the dynamo model with a geomagnetic composite [*Constable and Johnson*, 2005], SINT [*Valet et al.*, 2005], and an f^{-2}-law prediction [*Courtillot and Le Mouel*, 1988]. Vertical reference lines are shown at periods of 20 kyr and 20 Myr.

[17] **Acknowledgments.** The authors thank Andrew Biggin and an anonymous reviewer.

[18] The Editor thanks Andrew Biggin and an anonymous reviewer.

References

Amit, H., R. Leonhardt, and J. Wicht (2010), Polarity reversals from paleomagnetic observations and numerical dynamo simulations, *Space Sci. Rev.*, *155*, 1–43, doi:10.1007/s11214-010-9695-2.

Aubert, J., S. Labrosse, and C. Poitou (2009), Modeling the paleo-evolution of the geodynamo, *Geophys. J. Int.*, *179*(3), 1414–1428, doi:10.1111/j.1365-246X.2009.04361.x.

Biggin, A., and D. Thomas (2003), Analysis of long-term variations in the geomagnetic poloidal field intensity and evaluation of their relationship with global geodynamics, *Geophys. J. Int.*, *152*(2), 392–415, doi:10.1046/j.1365-246X.2003.01849.x.

Biggin, A., D. van Hinsbergen, C. Langereis, G. Straathof, and M. Deenen (2008), Geomagnetic secular variation in the Cretaceous Normal Superchron and in the Jurassic, *Phys. Earth Planet. Inter.*, *169*(1–4), 3–19, doi:10.1016/j.pepi.2008.07.004.

Cande, S. C., and D. V. Kent (1995), Revised calibration of the geomagnetic polarity timescale for the Late Cretaceous and Cenozoic, *J. Geophys. Res.*, *100*(B4), 6093–6095, doi:10.1029/94JB03098.

Christensen, U., and J. Aubert (2006), Scaling properties of convection-driven dynamos in rotating spherical shells and application to planetary magnetic fields, *Geophys. J. Int.*, *166*(1), 97–114, doi:10.1111/j.1365-246X.2006.03009.x.

Constable, C. (2000), On rates of occurrence of geomagnetic reversals, *Phys. Earth Planet. Inter.*, *118*(3), 181–193.

Constable, C., and C. Johnson (2005), A paleomagnetic power spectrum, *Phys. Earth Planet. Inter.*, *153*(1–3), 61–73, doi:10.1016/j.pepi.2005.03.015.

Constable, C. G., L. Tauxe, and R. L. Parker (1998), Analysis of 11 Myr of geomagnetic intensity variation, *J. Geophys. Res.*, *103*(B8), 17,735–17,748.

Courtillot, V., and J. Le Mouel (1988), Time variations of the Earth's magnetic field: From daily to secular, *Annu. Rev. Earth Planet. Sci.*, *16*(1), 389–476.

Driscoll, P., and P. Olson (2009a), Effects of buoyancy and rotation on the polarity reversal frequency of gravitationally driven numerical dynamos, *Geophys. J. Int.*, *178*(3), 1337–1350, doi:10.1111/j.1365-246X.2009.04234.x.

Driscoll, P., and P. Olson (2009b), Polarity reversals in geodynamo models with core evolution, *Earth Planet. Sci. Lett.*, *282*(1–4), 24–33, doi:10.1016/j.epsl.2009.02.017.

Gallet, Y., and V. Courtillot (1995), Geomagnetic reversal behaviour since 100 Ma, *Phys. Earth Planet. Inter.*, *92*(3), 235–244.

Gallet, Y., J. Besse, L. Krystyn, J. Marcoux, and H. Théveniaut (1992), Magnetostratigraphy of the late Triassic Bolücektasi Tepe section (southwestern Turkey): Implications for changes in magnetic reversal frequency, *Phys. Earth Planet. Inter.*, *73*(1–2), 85–108.

Hulot, G., and Y. Gallet (2003), Do superchrons occur without any palaeomagnetic warning?, *Earth Planet. Sci. Lett.*, *210*(1–2), 191–201, doi:10.1016/S0012-821X(03)00130-4.

Jonkers, A. (2007), Discrete scale invariance connects geodynamo timescales, *Geophys. J. Int.*, *171*(2), 581–593, doi:10.1111/j.1365-246X.2007.03551.x.

Lowrie, W., and D. Kent (2004), Geomagnetic polarity timescales and reversal frequency regimes, in *Chapman Conference on Timescales of the Internal Geomagnetic Field, Gainesville, Florida*, *Geophys. Monogr. Ser.*, vol. 145, pp. 117–129, AGU, Washington, D. C.

McFadden, P., and R. Merrill (1997), Asymmetry in the reversal rate before and after the Cretaceous Normal Polarity Superchron, *Earth Planet. Sci. Lett.*, *149*(1–4), 43–47.

Nakagawa, T., and P. J. Tackley (2005), Deep mantle heat flow and thermal evolution of the Earth's core in thermochemical multiphase models of mantle convection, *Geochem. Geophys. Geosyst.*, *6*, Q08003, doi:10.1029/2005GC000967.

Olson, P., G. Schubert, and C. Anderson (1987), Plume formation in the D″-layer and the roughness of the core-mantle boundary, *Nature*, *327*, 409–413.

Olson, P. L., R. S. Coe, P. E. Driscoll, G. A. Glatzmaier, and P. H. Roberts (2010), Geodynamo reversal frequency and heterogeneous core-mantle boundary heat flow, *Phys. Earth Planet. Inter.*, *180*(1–2), 66–79, doi:10.1016/j.pepi.2010.02.010.

Pavlov, V., and Y. Gallet (2005), A third superchron during the early Paleozoic, *Episodes*, *28*(2), 78–84.

Roberts, P., and G. Glatzmaier (2001), The geodynamo, past, present and future, *Geophys. Astrophys. Fluid Dyn.*, *94*(1), 47–84.

Ryan, D. A., and G. R. Sarson (2007), Are geomagnetic field reversals controlled by turbulence within the Earth's core?, *Geophys. Res. Lett.*, *34*, L02307, doi:10.1029/2006GL028291.

Tarduno, J., R. Cottrell, and A. Smirnov (2001), High geomagnetic intensity during the mid-Cretaceous from Thellier analyses of single plagioclase crystals, *Science*, *291*(5509), 1779–1783.

Tauxe, L., and T. Yamazaki (2007), Paleointensities, in *Treatise on Ge physics*, vol. 5 *Geomagnetism*, edited by G. Schubert, chap. 13, pp. 509–563, Elsevier, Amsterdam.

Valet, J., L. Meynadier, and Y. Guyodo (2005), Geomagnetic field strength and reversal rate over the past 2 Million years, *Nature*, *435*, 802–805, doi:10.1038/nature03674.

Zhong, S., N. Zhang, Z. Li, and J. Roberts (2007), Supercontinent cycles, true polar wander, and very long-wavelength mantle convection, *Earth Planet. Sci. Lett.*, *261*(3–4), 551–564, doi:10.1016/j.epsl.2007.07.049.

P. Driscoll, Geology and Geophysics, Yale University, New Haven, CT 06511, USA. (peter.driscoll@yale.edu)

P. Olson, Earth and Planetary Science, Johns Hopkins University, Baltimore, MD 21218, USA.